ACCOUNTS of chemical research

Article

pubs.acs.org/accounts

Pyridine Coordination Chemistry for Molecular Assemblies on Surfaces

Graham de Ruiter, Michal Lahav, and Milko E. van der Boom*

Department of Organic Chemistry, The Weizmann Institute of Science, 7610001 Rehovot, Israel

CONSPECTUS: Since the first description of coordination complexes, many types of metal−ligand interactions have creatively been used in the chemical sciences. The rich coordination chemistry of pyridine-type ligands has contributed significantly to the incorporation of diverse metal ions into functional materials. Here we discuss molecular assemblies (MAs) formed with a variety of pyridine-type compounds and a metal containing cross-linker (e.g., $PdCl_2(PhCN_2)$). These MAs are formed using Layer-by-Layer (LbL) deposition from solution that allows for precise fitting of the assembly properties through molecular programming. The position of each component can be controlled by altering the assembly sequence, while the degree of intermolecular interactions can be varied by the level of π-conjugation and the availability of metal coordination sites. By setting the structural parameters (e.g., bond angles, number of coordination sites, geometry) of the ligand, control over MA structure was achieved, resulting in surface-confined metal−organic networks and oligomers. Unlike MAs that are constructed with organic ligands, MAs with polypyridyl complexes of ruthenium, osmium, and cobalt are active participants in their own formation and amplify the growth of the incoming molecular layer. Such a self-propagating behavior for molecular systems is rare, and the mechanism of their formation will be discussed. These exponentially growing MAs are capable of storing metal salts that can be used during the buildup of additional molecular layers. Various parameters influencing the film growth mechanism will be presented, including (i) the number of binding sites and geometry of the organic ligands, (ii) the metal and the structure of the polypyridyl complexes, (iii) the influence of the metal cross-linker (e.g., second or third row transition metals), and (iv) the deposition conditions. By systematic variation of these parameters, switching between linear and exponential growth could be demonstrated for MAs containing structurally well-defined polypyridyl complexes. The porosity of the MAs has been estimated by using electrochemically active probes. Incorporating multiple polypyridyl complexes of osmium and ruthenium into a single assembly give rise to composite materials that exhibit interesting electrochemical and electrochromic properties. These functional composites are especially attractive as they exhibit properties that neither of each metal complex possesses individually. Some of our MAs have very high coloration efficiencies, redox stability, fast responsive times and operate at voltages < 1.5 V. Moreover, their electrochemical properties are dependent on the deposition sequence of the polypyridyl complexes, resulting in MAs that possesses distinctive electron transfer pathways. Finally, some of these MAs are described in terms of their practical applications in electrochromic materials, storage-release chemistry, solar cells, and electron transport properties.

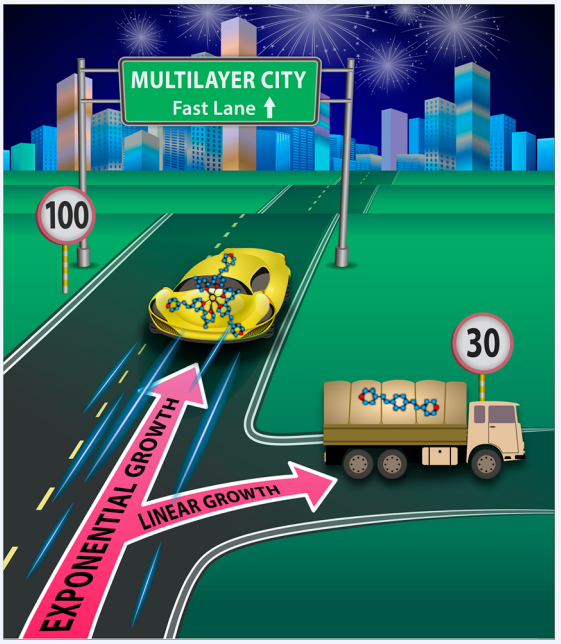

I. INTRODUCTION

Solution-based deposition of molecular building blocks offers the possibility of forming multicomponent materials in an organized manner.[1] Different functionalities can be introduced at various stages of the assembly process with control over the molecular arrangement.[2] Seminal studies on Layer-by-Layer (LbL) assemblies using metal−ligand coordination appeared in the literature during the 1990s and include works by the groups of Mallouk, Ulman, Katz, and Rubinstein.[2−5] In 2006 we used pyridine-coordination chemistry to generate oligomers on surfaces.[6] The groups of Wöll, Fischer, Nishihara, and Kitigawa recently reported molecular assemblies (MAs) with a remarkable versatility.[7−11] For instance, Nishihara elegantly developed the concept of molecular programming by constructing large molecular wires with terpyridine complexes of Fe and Co.[10] The structure and the properties of such materials are still difficult to control and predict *a priori*, due to several factors, including control over intermolecular interactions, packing, and molecular orientation. Notwithstanding, this highly general and versatile approach permits the synthesis

Received: March 14, 2014
Published: October 28, 2014

Scheme 1. Overview of the Molecular Components Used in Forming the Molecular Assemblies (MAs 1−10)[6,15−27a]

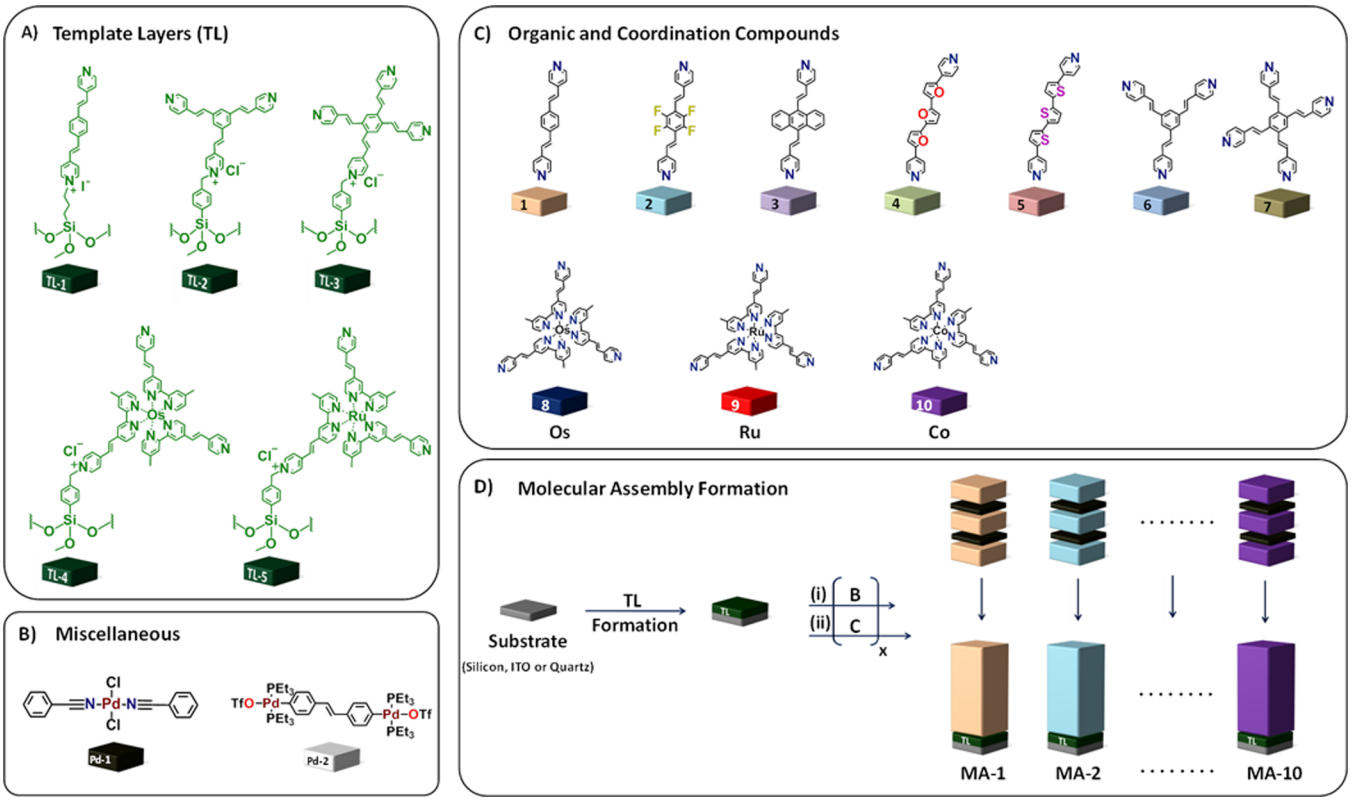

[a](A) Pyridyl-terminated template layers (TL **1**−**5**) formed from compounds **1** and **6**−**9**, respectively. (B) Molecular structure of $PdCl_2(PhCN)_2$ (Pd-**1**) and a bimetallic complex (Pd-**2**) used for crosslinking compounds **1**−**10**. (C) Organic (**1**−**7**) and coordination compounds (**8**−**10**) used for fabricating molecular assemblies (MAs). (D) Schematic representation of the formation of MAs **1**−**10** using an iterative deposition procedure with compounds **1**−**10** and Pd-**1**, or **1**, **3** with Pd-**2**. The charges of the osmium, ruthenium and cobalt complexes and the PF_6^- anions have been omitted.

and study of new molecular assemblies (MAs) that have nanometer-level precision in their molecular arrangement.[12,13]

In this Account, we discuss our strategy for assembling surface-bound materials, which involves a solution-based deposition procedure (Scheme 1).[6] Our strategy relies on the coordination chemistry of a d^8 metal salt such as $PdCl_2(PhCN)_2$ with pyridine-type ligands. Owing to the large library of pyridine- and bipyridine-type compounds, together with their rich coordination chemistry,[14] our approach resulted in different types of MAs having an array of material properties. The emerging synergism between the molecular building blocks and the different types of MAs becomes apparent as different growth mechanisms (linear vs exponential)[15,16] and assembly sequences are evaluated.[12,13]

II. SELF-ASSEMBLY OF ORGANIC COMPOUNDS ON SURFACES

The structural directionality imposed by metal salts upon coordination with organic linkers has led to a variety of assemblies on surfaces.[14] The square-planar coordination geometry of palladium(II), and in particular, the *trans* coordination chemistry, ensures linear propagation of the MAs.[6] The structural similarity of compounds **1**−**3** enabled us to systematically study the effect of fluorination or extension of the aromatic core on the assembly.[6,17,21] MAs **1**−**3** were formed according to the deposition method outlined in Scheme 1. These MAs exhibited regular and linear growth. The orientation of the chromophores inside the MAs is most likely dictated by the structure of the template layer (TL-**1**), which is at an ∼20° angle with respect to the surface plane. This orientation might result from hybridization of the benzylic carbon atom (19°) in the TL, that is propagated by the linear *trans* coordination chemistry of Pd.[6] As a result, the thickness increases by ∼34% of the chromophore length in each deposition step. Such template layer-dependent angular growth was also observed recently by Dinolfo and Schalley upon deposition of large macrocycles and porphyrins.[28,29] MA-**1** and MA-**2** each exhibit optical properties that are characteristic for compounds **1** and **2**, whereas MA-**3** is the exception due to strong intermolecular interactions.[17] The 30° twist angle of the anthracene core, with respect to vinylpyridine, allows for face-to-face interactions between the π-conjugated systems, during the axial growth of the MAs (Figure 1). The observed 3D order for MA-**3**, induced by intermolecular interactions, was demonstrated by X-ray reflectivity (XRR) and UV/vis measurements. Examples of crystalline thin films by solution-based deposition have been reported by the groups of Kitagawa, Wöll, and Fisher.[7,8]

Such a 3D order is absent in MA-**1** and MA-**2**, although for MA-**1** formation of J-aggregates is observed.[6] Despite these aggregates, the intermolecular interactions in MA-**1** are far less pronounced than in the MA-**3**. The use of a fluorinated aromatic core leads to a further decrease in intermolecular interactions.[21] MAs with the partially fluorinated compound **2** exhibited a smooth surface and large grains and a low index of refraction.[21] This might be due to different packing in MA-**2**, which is consistent with the observation of Gierschner et al.

dx.doi.org/10.1021/ar500112b | Acc. Chem. Res. 2014, 47, 3407−3416

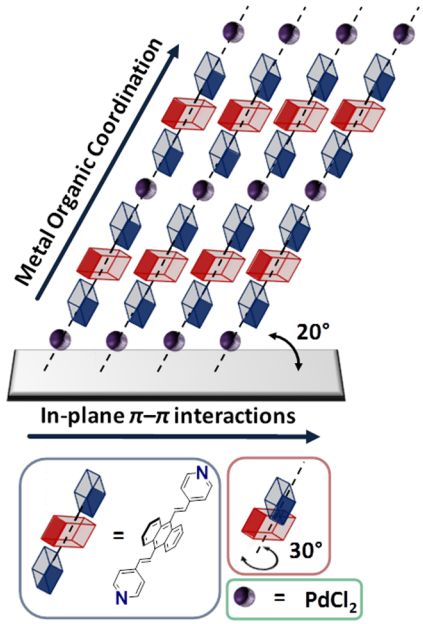

Figure 1. Schematic representation of the 3D-ordered molecular assembly.[17] The axial growing assemblies were formed by an alternating deposition of chromophore **3** with $PdCl_2(PhCN)_2$ (Pd-**1**) (Scheme 1). The in-plane π–π interactions are induced by the anthracene moieties.

that demonstrated a facial-to-edge herringbone packing for **1** and a face-to-face arrangement for **2**.[30]

The scope of our assembly strategy was demonstrated by substituting $PdCl_2(PhCN)_2$ (Pd-**1**) for a bimetallic organometallic complex (Pd-**2**).[19] This complex forms in combination with compounds **1** and **3** positively charged constructs MA-**1b** and MA-**3b**, respectively. Density functional theory (DFT) calculations of the oligomers revealed that the positive charges are localized on the Pd centers (Figure 2). Apparently, there is

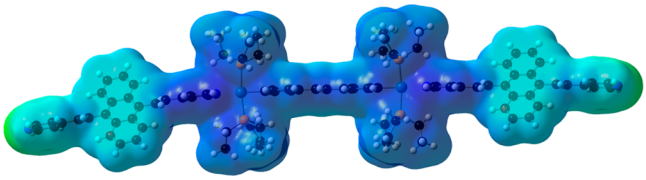

Figure 2. Dimers of chromophore **3** with bimetallic palladium complex Pd-**2**.[19] The electron density profile shows that the positive charges are mostly concentrated on the palladium and phosphine atoms (dark blue).

no electron delocalization along the oligomers. Although linear growing MAs were formed, the structural components remain electronically isolated. Although strong intermolecular interactions between the oligomer chains have been observed for MA-**1** or MA-**3**, for MA-**1b** and MA-**3b** these interactions are absent. The absence of apparent interactions between oligomers MA-**1b** and MA-**3b** can be attributed to the bulkiness of the triethylphosphine ligands.

Bendikov and co-workers introduced various polyselenophenes and long oligofurans (coined Bendimers).[31,32] The presence of large π-conjugated systems with heteroatoms is especially attractive for organic electronics. In particular, these oligofurans are of special interest because they exhibit properties similar to those of oligothiophenes.[33] We compared the molecular properties of assemblies MA-**4** and MA-**5**, which were constructed with derivatives of terthiophene and terfuran (**4** and **5**).[27] The electrochemical investigation reveals some cooperative effects in MA-**4** and MA-**5**, where thickness-dependent oxidation processes were observed. The electron density for MA-**4** was higher than that in MA-**5** due to the different packing of **4** and **5** in the MAs. No apparent intermolecular interactions among the oligofurans and oligothiophenes were detected. Interestingly, these studies indicated that the differences between MA-**4** and MA-**5** are subtle.

So far, we discussed organic chromophores (**1**–**5**) with two pyridine moieties.[6,17,19,21,27] The ability to form extended networks, upon increasing the number of pyridine moieties, has been explored as well.[15,23] Stang et al. showed that molecular rectangles on Au surfaces can be formed having a long-range order with a virtually defect-free topology.[34] These rectangles exhibit an in-plane orientation with respect to the Au surface. In contrast to the in-plane assembly, we demonstrated growth perpendicular to the surface with compounds **6** and **7** (MA-**6** and MA-**7**). A linear-type growth was observed with a constant molecular density.[15,23] In each deposition, a similar amount of chromophore **6** or **7** is added to the assembly. A dendritic type of growth with a concomitant increase in the electron density upon each deposition step does not occur. The XPS derived nitrogen-to-metal ratio revealed the formation of coordinatively saturated metal–organic networks (MONs).[23] Energy minimization with the semiempirical Parametric Method 6 (PM6) resulted in several structures of $PdCl_2$ with compounds **6** and **7**. Of particular interest is the planar hexamer composed of compound **6**, which exhibits C_{6h} symmetry (Figure 3A); extension of these monomers led to the formation of honeycomb-like structures, with large 3.5 nm Pd–Pd intermolecular spacings or pores. Owing to a different geometry, the calculated minimum energy structure with

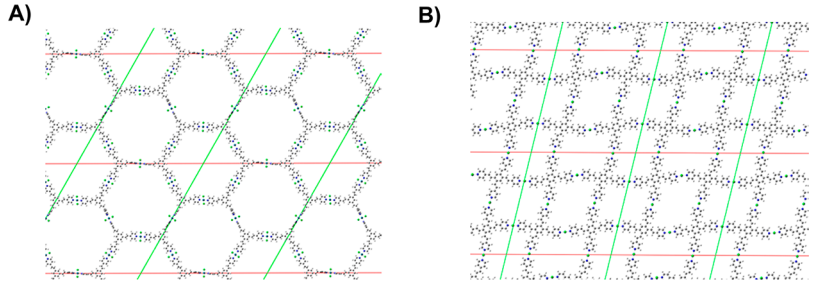

Figure 3. Computationally optimized network of compounds **6** (A) and **7** (B) with $PdCl_2$ according to the semiempirical method (PM6). The cross-ring Pd distances are 3.5 nm (A) and 1.7 and 2.2 nm (B). Reproduced with permission from ref 23. Copyright 2010 American Chemical Society.

dx.doi.org/10.1021/ar500112b | Acc. Chem. Res. 2014, 47, 3407–3416

compound **7** and $PdCl_2$ is a parallelogram-type structure. The unsymmetrical nature of a parallelogram gives rise to two different types of pores, with intermolecular Pd−Pd spacings of 2.2 nm (horizontal) and 1.7 nm (vertical), respectively (Figure 3B). Electrochemical studies with a bulky quinone (2,6-di-*tert*-butylcyclohexa-2,5-diene-1,4-dione) and MA-**6** confirmed the formation of porous structures as indicated computationally.[23]

III. SELF-ASSEMBLY OF COORDINATION COMPOUNDS ON SURFACES

Incorporating structurally well-defined and redox-active metal complexes introduces useful functionalities to the MAs, including electrochromic,[12,20,22] electronic,[9,10,35−37] and catalytic properties.[38] By using multiple metal complexes, multi-stimuli-responsive materials can be generated. Such superposition of molecular properties in MAs was observed by Schmehl and Liang, who assembled complexes of Fe and Ru on the surface.[39] The assembly of polypyridyl and related complexes on the surface has been demonstrated by others as well.[9,10,35−37,39,40]

Our group mainly used polypyridyl complexes of Group 8 metals for the formation of redox-active MAs (Scheme 1).[12,13,15,16,18,20,22,24−26,41] These complexes were chosen due to their stability, iso-structurality, and isoelectronic nature, as well as for their electrochromic properties.[12,20,22] Our initial investigation focused on osmium complex **8** and the resulting MA-**8**.[18] Interestingly, the scaling of the molecular properties of MAs **8** is exponential. Such exponential growth is in sharp contrast with the linear growth observed for MAs **1**−**7**. Exponential growth of molecular architectures is rare and involves the use of branched ligands and/or metal complexes.[2,36] The branching allows for dendritic-type growth that scales with x^n, with x being the number of branches and n being the number of deposition steps. For this type of growth, the molecular density is expected to increase with each deposition step, whereas the thickness exhibits a regular and constant increase.[42] For our MAs, the mechanism of the exponential growth is fundamentally different. Diffusion processes might be operating akin to the mechanism for exponentially growing polyelectrolytes.[15,26,43] The following mechanism is most likely operating: Upon immersion of the MAs into a solution of $PdCl_2(PhCN)_2$, the Pd diffuses inside the MA and remains there during the film formation (Figure 4). The diffusion of Pd might occur in distinct diffusion domains, that contains a large excess of Pd homogeneously distributed throughout the film.[15,18] However, during immersion in a solution of chromophore **8**, the "trapped" Pd diffuses outward and aids the coordination of compound **8**, beyond a single molecular layer. Since upon each deposition the film thickness is increasing, and hence more palladium can be stored inside the larger diffusion domains, the observed growth of our MAs is exponential.

Support for such a mechanism is based on the following observations: (i) Unlike dendritic growth, the electron density profiles obtained for our MAs show a constant electron density as a function of the thickness (Figure 5A),[16,18] consistent with a homogeneous distribution of chromophore **8** and $PdCl_2(PhCN)_2$ throughout the assembly. (ii) XPS analysis of our MAs revealed that, after exposing the MAs to a solution of $PdCl_2(PhCN)_2$, the Pd/Os ratio is approximately 2× higher than expected and is independent of the angle of incidence of the X-ray beam, suggesting the presence of diffusion domains. However, when the MAs are exposed to the chromophore

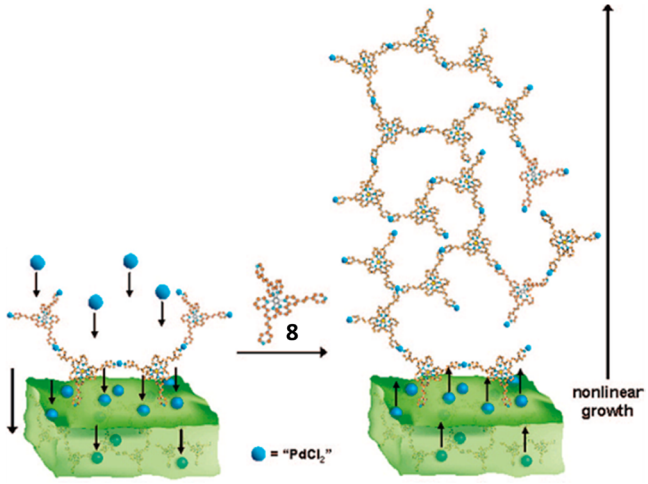

Figure 4. Schematic representation of the exponential growth of **8** and $PdCl_2(PhCN)_2$. Reproduced with permission from refs 15 and 18. Copyright 2010 and 2008 American Chemical Society.

solution (**8**), the Pd/Os ratio decreases in these diffusion domains, although some excess of Pd remains (Figure 5B).[15,18] (iii) The exposure time of the MAs to $PdCl_2(PhCN)_2$ is critical for exponential scaling of the molecular properties (Figure 5C).[15] Short exposure time (5 min) leads to linear growth of the MAs. Long exposure time (15 min) leads to exponential growth, and (iv) exponential scaling of the thickness was observed for all MAs (Figure 5D). These latter observations show that MAs can be designed to grow linearly or exponentially depending on the applied reaction environment. In contrast to linear growing MAs, the exponential growing MAs have an active role in their formation by storing the cross-linking component.

To evaluate the porosity of MA-**9**, electrochemical experiments were carried out with a series of quinones (**11**−**13**) (Figure 6; dashed traces).[25] These probes were chosen because their redox chemistry does not interfere with the $Ru^{2+/3+}$ redox couple. The relatively small quinones **11** and **12** are able to penetrate MAs having a thickness of 20 nm as indicated by the clear oxidation/reduction waves (Figure 6; solid traces). However, thickness-dependent redox chemistry was observed with MA-**9**. Whereas for 5.0 nm thick assemblies, quinone **13** was able to reach the surface of the ITO electrode, and no penetration was observed for a 20 nm thick assembly. The deduced pore size of MA-**9** lies somewhere between the size of quinones **12** and **13**.

The MA growth is also a function of the reactivity of the metal salts.[16] The labile benzonitrile ligands of $PdCl_2(PhCN)_2$ allow the incoming pyridine moieties of compounds **8**−**10** to be easily coordinated. The binding strength of the coordinating ligand in the $PdCl_2$ precursor influences the growth behavior of the MAs. The larger the binding strength toward Pd, the smaller and less pronounced is the exponential growth of the MAs (Figure 7A). Consequently, the growth of the MA-**9** is in the order $PdCl_2(PhCN)_2$ > $PdCl_2(COD)$ > $PdCl_2(SMe_2)_2$. A similar order is observed for platinum complexes of the type $PtX_2(PhCN)_2$, where X = Cl, Br, or I. The observed growth of the MAs is in the order of $PtI_2(PhCN)_2$ > $PtBr_2(PhCN)_2$ ≥ $PtCl_2(PhCN)_2$ (Figure 7B). These results are consistent with the fact that the size of the anion influences ligand exchange processes. The growth of MAs with $PdCl_2(PhCN)_2$ and $PtCl_2(PhCN)_2$ is also remarkably different. Apparently, the

dx.doi.org/10.1021/ar500112b | *Acc. Chem. Res.* 2014, 47, 3407−3416

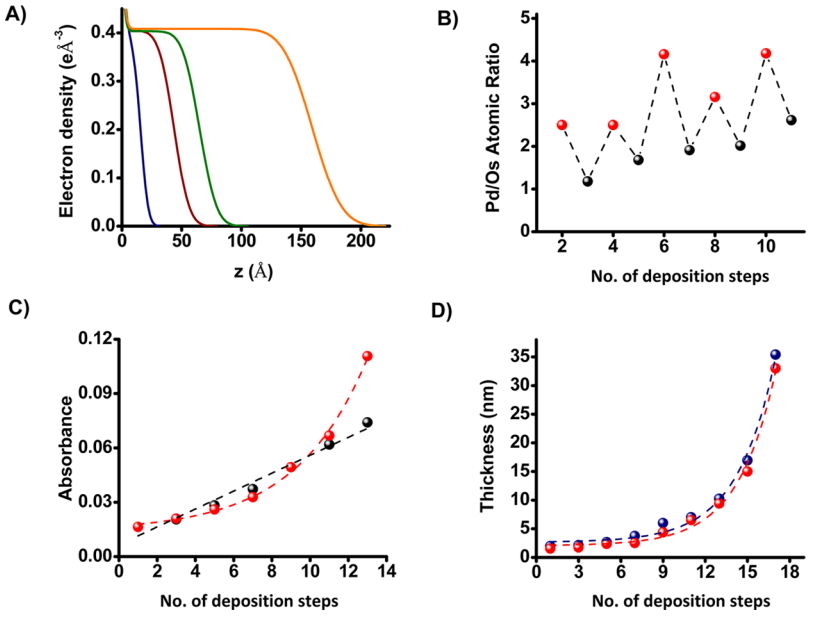

Figure 5. Representative characterization data of MA-**8**.[15,18] (A) Electron density profiles with thicknesses of 2 nm (blue trace), 6 nm (brown trace), 7 nm (green trace), and 17 nm (orange trace). (B) XPS-derived Pd/Os atomic ratios as a function of the number of deposition steps. The red dots indicate MAs that were last exposed to $(PdCl_2(PhCN)_2)$, whereas the black dots indicate MAs that were last exposed to **8**. (C) Linear or exponential dependence of the optical absorption of the metal-to-ligand charge transfer (MLCT), with MAs generated with a phenanthroline derivative of **8**, upon immersing the MAs in $PdCl_2(PhCN)_2$ for 5 min (black dots) or 15 min (red dots), respectively. (D) Exponential dependence of the XRR (blue dots) and ellipsometry (red dots) derived thickness. Reproduced with permission from refs 15 and 18. Copyright 2010 and 2008 American Chemical Society.

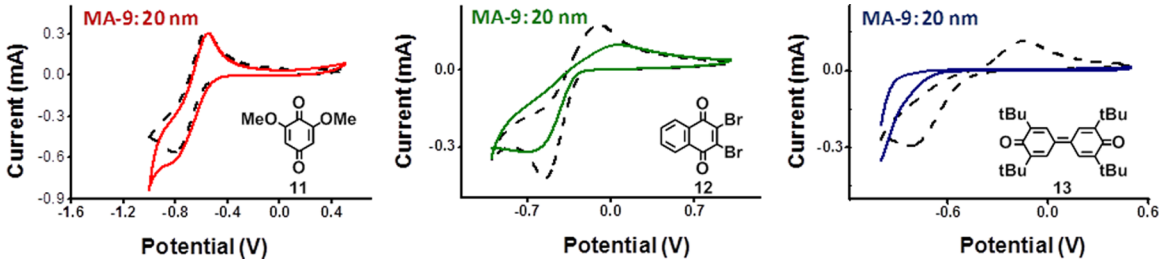

Figure 6. Representative cyclic voltammograms of quinones **11** (red traces), **12** (green traces), and **13** (blue traces) recorded with MA-**9**-functionalized ITO electrodes (20.0 nm) at a scan rate of 100 mV s^{-1}. The black dashed lines represent the voltammetric responses of the quinones using bare ITO electrodes. Reproduced with permission from ref 26. Copyright 2011 American Chemical Society.

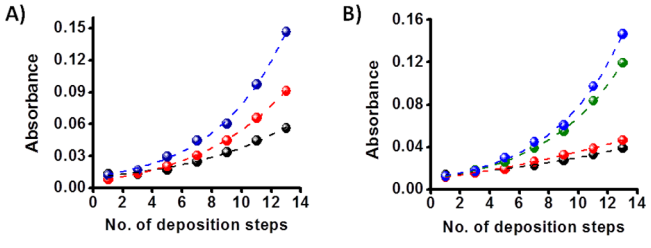

Figure 7. Different growth characteristics of MA-**9**, as monitored by the intensity metal–ligand charge transfer (MLCT) bands at λ = 495, as a function of (A) the coordinating ligands in $PdCl_2(L)_n$, where L = benzonitrile (n = 2, PhCN; blue circle), cyclooctadiene (n = 1, COD; red circle), and dimethylsulfide (n = 2, SMe_2; black circle), and (B) as a function of the anions in $PdX_2(L)_n$, where X = Cl (black circle), Br (red circle), or I (green circle). For a comparison, $PdCl_2(PhCN)_2$ (blue circle) is shown as well. All R^2 > 0.99. Reproduced with permission from ref 16. Copyright 2012 Royal Society of Chemistry.

Pd or Pt metal center has a significant effect on the benzonitrile ligand exchange.

IV. SEQUENCE-DEPENDENT ASSEMBLY ON SURFACES

The formation of our MAs with one kind of polypyridyl complex comprises of a deposition sequence whereby each deposition of a metal complex (Os, Ru, or Co) is followed by the deposition of a palladium or platinum salt. Several assembly sequences are possible when different metal complexes are used (Scheme 2).[12,13] Changing the deposition sequence of redox-active complexes result in assemblies with different electrochemical and electrochromic properties. These differences arise due to distinctive electron transfer pathways. We established a relationship between the assembly sequence and the electrochemical properties of the MAs with compounds **8** and **9**.[12,13] By using sequence-dependent assembly (SDA), it was found that the structure, thickness, and composition for multicomponent MA-**11**–**13** are similar and comparable to those of MA-**8** and MA-**9** (Schemes 1 and 2). However, electrochemically MA-**11**–**13** are completely different.

For MA-**11**, reversible behavior is observed for the $Os^{2+/3+}$ and $Ru^{2+/3+}$ redox couples, up to a thickness of 54 nm (Figure

dx.doi.org/10.1021/ar500112b | Acc. Chem. Res. 2014, 47, 3407–3416

Scheme 2. [a]

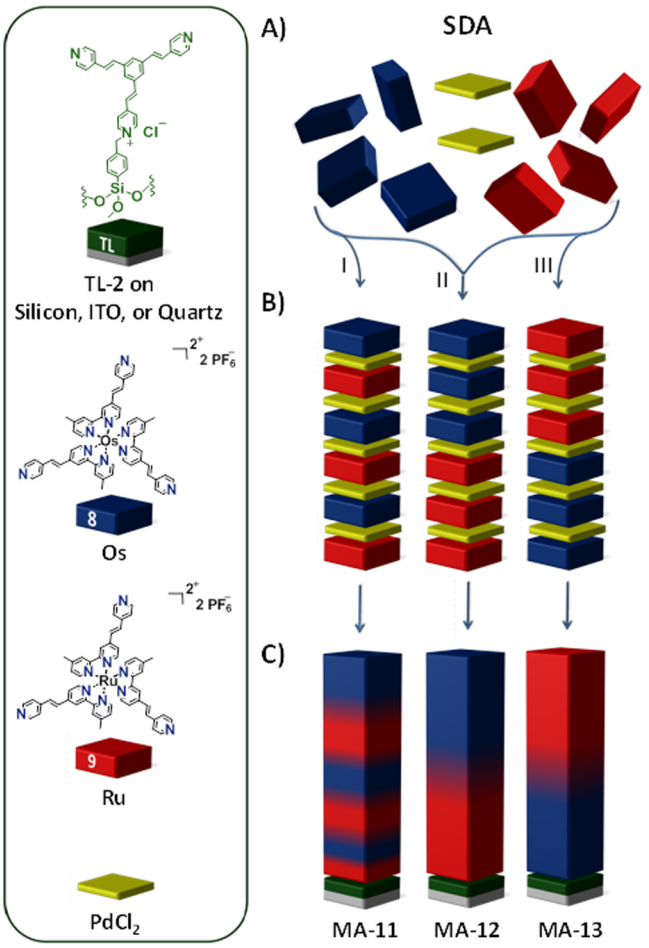

[a]Schematic overview of the formation of the molecular assemblies using Os (**8**) and Ru (**9**) complexes (A).[12,13] The sequence-dependent assembly (SDA) determines in which order the molecular components are deposited (B), resulting in MAs with a different distribution of the Os and Ru complexes **8** and **9** (C). Reproduced with permission from ref 12. Copyright 2013 American Chemical Society.

8A). In contrast, for MA-**12** and MA-**13**, the electrons can also be transferred from or to the outer layer by a unidirectional oxidative or reductive catalytic process. An oxidative catalytic prewave is observed for the Os metal center if the Ru thickness exceeds a threshold value (8.0 nm) in MA-**12** (Figure 8B). A reductive catalytic prewave for the Ru metal center occurs when the Os thickness exceeds a threshold value of 6.1 nm in MA-**13** (Figure 8C). Below these threshold values, reversible behavior is observed for both the $Os^{2+/3+}$ and $Ru^{2+/3+}$ redox couples.

The presence of catalytic prewaves is consistent with the observations of Murray et al. with bilayered polymers of Os and Ru.[44] For such systems, the electrochemical behavior can be described by (i) direct electron transfer—at low thicknesses—between the ITO electrode and the Os/Ru layers, which might be facilitated by the porosity and/or defects inside the MA, or (ii) indirect electron transfer—at higher thicknesses—where the metal-centers in the inner layer form a conductive path for the oxidation/reduction of the outer layer. In the latter case, the communication between the ITO electrode and the outer layer is blocked. Therefore, only at the onset potential of the Ru oxidation, oxidization of the outer Os layer occurs. Pathway (ii) seems to be dominant in MA-**12** and MA-**13**, whereas for MA-**11**, pathway (i) is prevailing (Scheme 3).

Not only are the molecular properties for complexes **8** and **9** cumulative, but also the organic chomophore **6** and complex **8** can be combined to construct multicomponent assemblies.[41] The ability of the osmium complex **8** to store palladium inside the porous networks enables the organic compound **6** to exhibit exponential growth as well. It is remarkable that the exponential growth of compound **6** is induced by **8**. Especially since exponential growth is not observed for MAs under the same reaction conditions with only compound **6**.[23] The exponential growth for the MA containing both **6** and **8** is less pronounced than for MAs with **8** only, and most likely attributed to a disruption in the diffusion domain inside the MA by **6**.

V. APPLICATION OF MAs ON THE SURFACE

MAs might be used for various applications, including resists on predetermined patterns to scale down larger parent structure obtained by electron-beam lithography.[45] Multivalued random access memory (RAM) was demonstrated using the electrochemically robust MA-**8**. Memory devices with optical readout that can store up to five states might be plausible. The read-write operations can be described by sequential logic circuits such as flip-flops and flip-flap-flops.[22] The application of complexes **8** and **9** in molecular Boolean logic and computing (MBLC) has been demonstrated, and discussed in two reviews.[46,47] Our MAs are also attractive electrochromic materials.[12,20,22] The optical response of the MLCT band is a function of the applied potential. For MA-**8**, consecutive modulation of the potential between 0.4 and 1.2 V switches its optical absorption intensity (Figure 9A). This process can be repeated more than 1000 times (Figure 9B). The coloration efficiency of 350 cm^2/C is high and comparable to that of

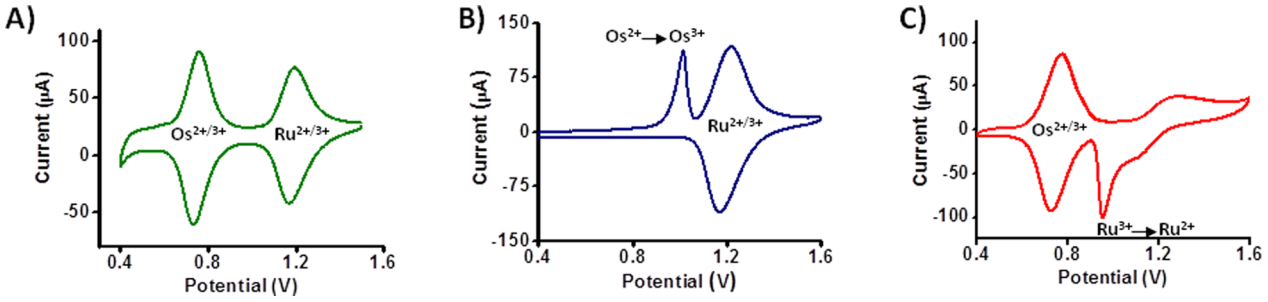

Figure 8. Cyclic voltammograms of MA-**11** (A), MA-**12** (B), and MA-**13** (C) on indium tin oxide (ITO) substrates, at a scan rate of 100 mV s^{-1}. The MAs were formed with compounds **8** and **9**, according to the sequence-dependent assembly (SDA) strategy outlined in Scheme 2. Reproduced with permission from ref 12. Copyright 2013 American Chemical Society.

dx.doi.org/10.1021/ar500112b | Acc. Chem. Res. 2014, 47, 3407−3416

Scheme 3. Overview of the Electron Transfer in MAs Constructed According to SDA II or III (Scheme 2)[a]

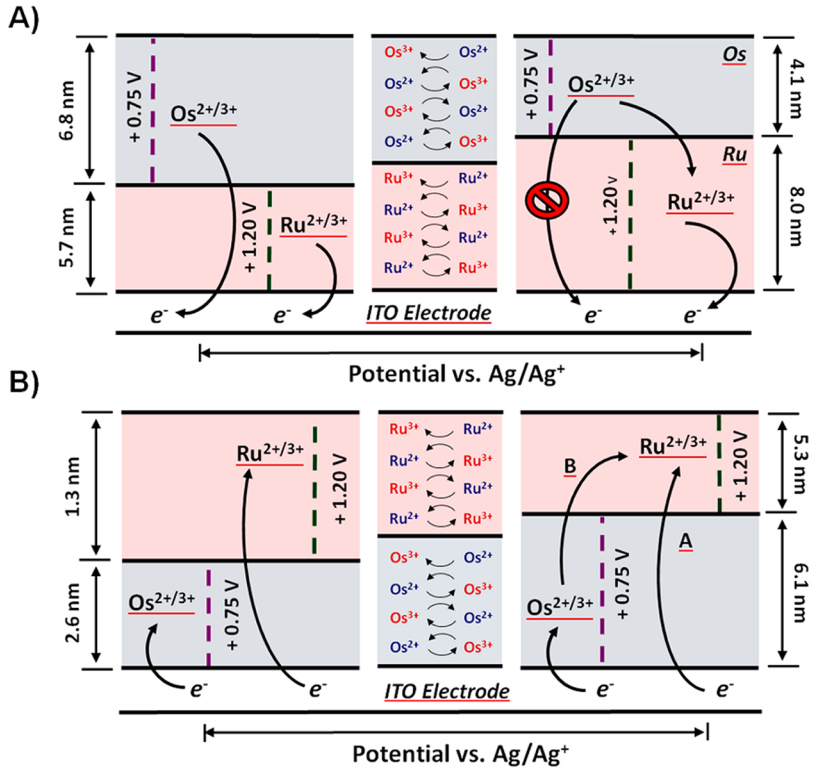

[a](A) Oxidative electron transfer in MA-**12**; above a threshold thickness of 8.0 nm, small amounts of Ru^{2+} are oxidized to Ru^{3+}, which allows the outer osmium layer to be oxidized. (B) Reductive electron transfer in MA-**13**. Reproduced with permission from ref 13. Copyright 2013 John Wiley and Sons.

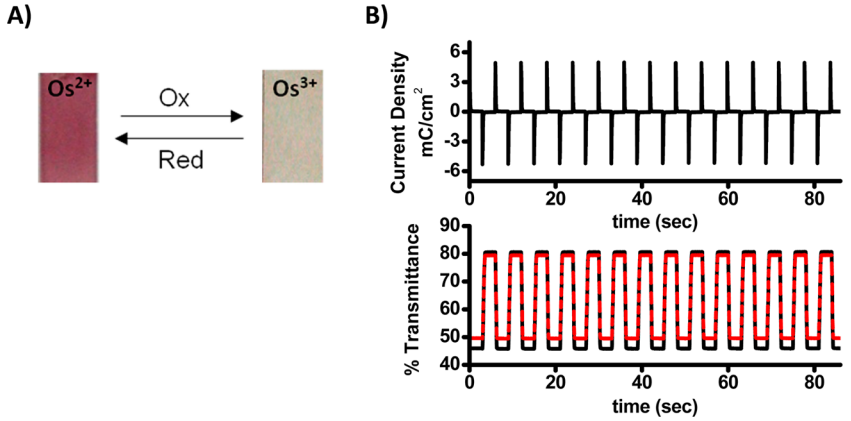

Figure 9. (A) Photographs of the reduced and oxidized ITO substrate coated with MA-**8**. (B) Switching current (top) and in situ transmittance (bottom) at λ = 510 nm with 3 s intervals, upon applying double potential steps (0.4 V − 1.2 V) in the chronoamperometric mode for MA-**8**. The red trace is the percent of transmittance after 1000 redox cycles. Reproduced with permission from ref 20. Copyright 2009 American Chemical Society.

PEDOT or its derivatives.[20] The contrast ratio (ΔT) is 35% for a 25 nm-thick assembly.

Furthermore, the MAs are suitable materials for the fabrication of solar cells.[25] Polypyridyl complexes of ruthenium have been extensively studied as light absorption materials. We used MA-**9** as an interlayer on the ITO electrode to facilitate electron transfer (Figure 10). The HOMO and LUMO energy levels for complex **9** matches well with the HOMO and LUMO levels of [6,6]-phenyl-C61-butyric acid methyl ester (PCBM) and poly(3-hexylthiophene) (P3HT), respectively. Inverted solar cells incorporating PCBM, P3HT, and MA-**9**, with a thickness ranging from 2.0 to 5.0 nm, displayed efficiencies as high as ∼3%.

VI. SUMMARY AND CONCLUSIONS

By using pyridine coordination chemistry with metal ions, we and others have shown that different and functional molecular assemblies (MAs) can be formed.[6,9,10,29,35−40,48] The discussed MAs allow for interface engineering and provides great control of the assembly properties. Each component can be positioned at a given distance from the inorganic surface, and by modifying the organic ligands intermolecular interactions can be directed.

dx.doi.org/10.1021/ar500112b | Acc. Chem. Res. 2014, 47, 3407−3416

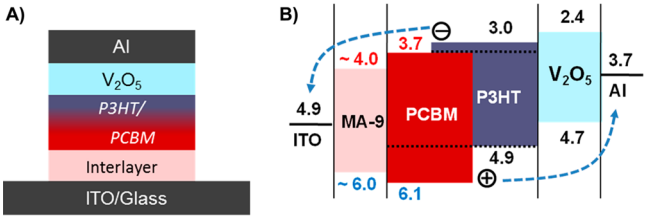

Figure 10. Structure (A) and energy level diagram (B; in eV) for the materials used in solar cell fabrication with [6,6]-phenyl-C61-butyric acid methyl ester (PCBM), poly(3-hexylthiophene) (P3HT), vanadium oxide (V_2O_5), and MA-**9**. Indium tin oxide (ITO) and aluminum (Al) were used as cathode and anode, respectively. Reproduced with permission from ref 25. Copyright 2010 American Chemical Society.

For fluorinated π-conjugated systems, minimal intermolecular interactions were found,[21] whereas by making use of large π-conjugated systems such as anthracene, 3D-organized structures were obtained.[17] Increasing the number of coordination sites leads to extended metal–organic networks.[23] We found that these MAs are structurally homogeneous and exhibit a linear type of growth. Moreover, we also demonstrated that exponential scaling of the assembly properties is obtained with polypyridyl complexes of Os, Ru, and Co.[15,16,18,24,41] This exponential growth includes storage of excess palladium inside the porous network. Furthermore, the assembly sequence of the polypyridyl complexes of Os and Ru can have drastic effects on the electrochemical properties.[12,13] To date, our self-propagating molecular assemblies have been used in designing solar cells, as well as in molecular logic, and electrochromic materials.[12,20,22] These materials exhibit better electrochromic properties than many inorganic films, and have a coloration efficiency and switching time comparable to industrially important conducting polymers. Yet many challenges remain. For instance, the role of the central metal ion is poorly understood in the self-propagating assembly of our MAs. Similarly, varying the counterion could lead to new materials with interesting properties. Recently, one-step assembly processes have been shown to be highly efficient for the formation of metal coordination based coatings.[49,50] Extending this strategy for our MAs might be applicable as well. As this field continues to develop, understanding the various parameters involved in MA formation might lead to more complex and ordered architectures displaying interesting functions such as the recently introduced SURMOFs and surface-confined homochiral helicates.[7,50] The controlled assembly of multiple components, combining their individual properties into a single assembly, is especially attractive.[12,13] Surfaces that display a molecular gradient are appealing, where the surface properties change in one, two, or three dimensions. However, the self-assembly of molecular gradients poses major challenges.

AUTHOR INFORMATION

Corresponding Author

*E-mail: milko.vanderboom@weizmann.ac.il.

Notes

The authors declare no competing financial interest.

Biographies

Graham de Ruiter obtained his B.Sc. (2006) and M.Sc. degrees (cum laude; 2008) in chemistry (working with Prof. Jan Reedijk) at Leiden University, The Netherlands. He received his Ph.D. degree in 2013 from the Weizmann Institute of Science (Israel), under the supervision of Prof. Milko van der Boom. Currently, he is a postdoctoral scholar at the California Institute of Technology with Prof. Theodor Agapie.

Michal Lahav received her B.Sc. in 1995 and Ph.D. degree in 2002 (Summa Cum Laude) in Chemistry from the Hebrew University of Jerusalem (Israel), working with Prof. Itamar Willner. She spent 2 years in the lab of Prof. Israel Rubinstein at the Weizmann Institute of Science in Israel, and 2 years in the group of Prof. George M. Whitesides at Harvard University as a postdoctoral fellow. She then joined the Department of Organic Chemistry at the Weizmann Institute of Science as an Associate Staff Scientist with Prof. Milko van der Boom.

Milko E. van der Boom received his B.Sc. degree (1992) in Chemical Engineering at the University of Applied Sciences in Amsterdam, The Netherlands, and a M.Sc. degree (1994) in Inorganic Chemistry at the University of Amsterdam (with Prof. Kees Elsevier). He earned his Ph.D. degree with distinction in 1999 from the Weizmann Institute of Science in Israel (with Prof. David Milstein). After 3 years of postdoctoral research with Prof. Tobin J. Marks at Northwestern University in the United States, he became a Faculty member in the Weizmann Institute's Department of Organic Chemistry, and holds the Bruce A. Pearlman Professorial Chair in Synthetic Organic Chemistry.

ACKNOWLEDGMENTS

This research was supported by the Helen and Martin Kimmel Center for Molecular Design, the Mary and Tom Beck-Canadian Center for Alternative Energy Research, David Rosenberg (Chicago, IL), the Yeda-Sela Center for Basic Research, a research grant from the Leona M. and Harry B. Helmsley Charitable Trust, and the Israel Science Foundation (ISF) Grant No. 289/09. We thank those who participated in the presented work. Their names can be found in the listed papers.

REFERENCES

(1) Hammond, P. T. Form and function in multilayer assembly: New applications at the nanoscale. *Adv. Mater.* **2004**, *16*, 1271–1293.
(2) Rubinstein, I.; Vaskevich, A. Self-assembly of nanostructures on surfaces using metal–organic coordination. *Isr. J. Chem.* **2010**, *50*, 333–346.
(3) Hong, H. G.; Mallouk, T. E. Electrochemical measurements of electron-transfer rates through zirconium 1,2-ethanediylbis-(phosphonate) multilayers films on gold electrodes. *Langmuir* **1991**, *7*, 2362–2369.
(4) Katz, H. E.; Scheller, G.; Putvinski, T. M.; Schilling, M. L.; Wilson, W. L.; Chidsey, C. E. D. Polar orientation of dyes in robust multilayers by zirconium phosphate-phosphonate interlayers. *Science* **1991**, *254*, 1485–1487.
(5) Evans, S. D.; Ulman, A.; Goppert-Berarducci, K. E.; Gerenser, L. J. Self-assembled multilayers of ω-mercaptoalkanoic acids: Selective ionic interactions. *J. Am. Chem. Soc.* **1991**, *113*, 5866–5868.
(6) Altman, M.; Shukla, A. D.; Zubkov, T.; Evmenenko, G.; Dutta, P.; van der Boom, M. E. Controlling structure from the bottom-up: Structural and optical properties of layer-by-layer assembled palladium coordination-based multilayers. *J. Am. Chem. Soc.* **2006**, *128*, 7374–7382.
(7) Shekhah, O.; Wang, H.; Paradinas, M.; Ocal, C.; Schupbach, B.; Terfort, A.; Zacher, D.; Fischer, R. A.; Wöll, C. Controlling interpenetration in metal-organic frameworks by liquid-phase epitaxy. *Nat. Mater.* **2009**, *8*, 481–484.

(8) Makiura, R.; Motoyama, S.; Umemura, Y.; Yamanaka, H.; Sakata, O.; Kitagawa, H. Surface nano-architecture of a metal-organic framework. *Nat. Mater.* **2010**, *9*, 565−571.
(9) Kurita, T.; Nishimori, Y.; Toshimitsu, F.; Muratsugu, S.; Kume, S.; Nishihara, H. Surface junction effects on the electron conduction of molecular wires. *J. Am. Chem. Soc.* **2010**, *132*, 4524−4525.
(10) Nishimori, Y.; Kanaizuka, K.; Kurita, T.; Nagatsu, T.; Segawa, Y.; Toshimitsu, F.; Muratsugu, S.; Utsuno, M.; Kume, S.; Murata, M.; Nishihara, H. Superior electron-transport ability of π-conjugated redox molecular wires prepared by the stepwise coordination method on a surface. *Chem.—Asian J.* **2009**, *4*, 1361−1367.
(11) Kanaizuka, K.; Haruki, R.; Sakata, O.; Yoshimoto, M.; Akita, Y.; Kitagawa, H. Construction of highly oriented crystalline surface coordination polymers composed of copper dithiooxamide complexes. *J. Am. Chem. Soc.* **2008**, *130*, 15778−15779.
(12) de Ruiter, G.; Lahav, M.; Evmenenko, G.; Dutta, P.; Cristaldi, D. A.; Gulino, A.; van der Boom, M. E. Composite molecular assemblies: Nanoscale structural control and spectroelectrochemical diversity. *J. Am. Chem. Soc.* **2013**, *135*, 16533−16544.
(13) de Ruiter, G.; Lahav, M.; Hodaya, K.; van der Boom, M. E. Sequence-dependent assembly to control molecular interface properties. *Angew. Chem., Int. Ed.* **2013**, *52*, 704−709.
(14) Northrop, B. H.; Zheng, Y. R.; Chi, K. W.; Stang, P. J. Self-organization in coordination-driven self-assembly. *Acc. Chem. Res.* **2009**, *42*, 1554−1563.
(15) Choudhury, J.; Kaminker, R.; Motiei, L.; de Ruiter, G.; Morozov, M.; Lupo, F.; Gulino, A.; van der Boom, M. E. Linear vs exponential formation of molecular-based assemblies. *J. Am. Chem. Soc.* **2010**, *132*, 9295−9297.
(16) Motiei, L.; Feller, M.; Evmenenko, G.; Dutta, P.; van der Boom, M. E. Controlling growth of self-propagating molecular assemblies. *Chem. Sci.* **2012**, *3*, 66−71.
(17) Altman, M.; Zenkina, O.; Evmenenko, G.; Dutta, P.; van der Boom, M. E. Molecular assembly of a 3D-ordered multilayer. *J. Am. Chem. Soc.* **2008**, *130*, 5040−5041.
(18) Motiei, L.; Altman, M.; Gupta, T.; Lupo, F.; Gulino, A.; Evmenenko, G.; Dutta, P.; van der Boom, M. E. Self-propagating assembly of a molecular-based multilayer. *J. Am. Chem. Soc.* **2008**, *130*, 8913−8914.
(19) Altman, M.; Zenkina, O. V.; Ichiki, T.; Iron, M. A.; Evmenenko, G.; Dutta, P.; van der Boom, M. E. Positive constructs: Charges localized on surface-confined organometallic oligomers. *Chem. Mater.* **2009**, *21*, 4676−4684.
(20) Motiei, L.; Lahav, M.; Freeman, D.; van der Boom, M. E. Electrochromic behavior of a self-propagating molecular-based assembly. *J. Am. Chem. Soc.* **2009**, *131*, 3468−3469.
(21) Altman, M.; Rachamim, M.; Ichiki, T.; Iron, M. A.; Evmenenko, G.; Dutta, P.; van der Boom, M. E. Designing surface-confined coordination oligomers. *Chem.—Eur. J.* **2010**, *16*, 6744−6747.
(22) de Ruiter, G.; Motiei, L.; Choudhury, J.; Oded, N.; van der Boom, M. E. Electrically addressable multistate volatile memory with flip-flop and flip-flap-flop logic circuits on a solid support. *Angew. Chem., Int. Ed.* **2010**, *49*, 4780−4783.
(23) Kaminker, R.; Motiei, L.; Gulino, A.; Fragalà, I.; Shimon, L. J. W.; Evmenenko, G.; Dutta, P.; Iron, M. A.; van der Boom, M. E. Stepwise assembly of coordination-based metal-organic networks. *J. Am. Chem. Soc.* **2010**, *132*, 14554−14561.
(24) Motiei, L.; Lahav, M.; Gulino, A.; Iron, M. A.; van der Boom, M. E. Electrochemical characteristics of a self-propagating molecular-based assembly. *J. Phys. Chem. B* **2010**, *114*, 14283−14286.
(25) Motiei, L.; Yao, Y.; Choudhury, J.; Yan, H.; Marks, T. J.; van der Boom, M. E.; Facchetti, A. Self-propagating molecular assemblies as interlayers for efficient inverted bulk-heterojunction solar cells. *J. Am. Chem. Soc.* **2010**, *132*, 12528−12530.
(26) Motiei, L.; Kaminker, R.; Sassi, M.; van der Boom, M. E. Molecule and electron transfer through coordination-based molecular assemblies. *J. Am. Chem. Soc.* **2011**, *133*, 14264−14266.
(27) Hayoun Barak, A.; de Ruiter, G.; Lahav, M.; Sharma, S.; Gidron, O.; Evmenenko, G.; Dutta, P.; Bendikov, M.; van der Boom, M. E. Coordination-based molecular assemblies of oligofurans and oligothiophenes. *Chem.—Eur. J.* **2013**, *19*, 8821−8831.
(28) Palomaki, P. K. B.; Dinolfo, P. H. Structural analysis of porphyrin multilayer films on ito assembled using copper(i)-catalyzed azide−alkyne cycloaddition by ATR IR. *ACS Appl. Mater. Interfaces* **2011**, *3*, 4703−4713.
(29) Richter, S.; Traulsen, C. H. H.; Heinrich, T.; Poppenberg, J.; Leppich, C.; Holzweber, M.; Unger, W. E. S.; Schalley, C. A. Sequence-programmable multicomponent multilayers of nanometer-sized tetralactam macrocycles on gold surfaces. *J. Phys. Chem. C* **2013**, *117*, 18980−18985.
(30) Gierschner, J.; Ehni, M.; Egelhaaf, H.-J.; Milián Medina, B.; Beljonne, D.; Benmansour, H.; Bazan, G. C. Solid-state optical properties of linear polyconjugated molecules: π-stack contra herringbone. *J. Chem. Phys.* **2005**, *123*, 144914−144918.
(31) Gidron, O.; Diskin-Posner, Y.; Bendikov, M. α-oligofurans. *J. Am. Chem. Soc.* **2010**, *132*, 2148−2150.
(32) Patra, A.; Wijsboom, Y. H.; Zade, S. S.; Li, M.; Sheynin, Y.; Leitus, G.; Bendikov, M. Poly(3,4-ethylenedioxyselenophene). *J. Am. Chem. Soc.* **2008**, *130*, 6734−6736.
(33) Gidron, O.; Varsano, N.; Shimon, L. J. W.; Leitus, G.; Bendikov, M. Study of a bifuran vs. bithiophene unit for the rational design of π-conjugated systems. What have we learned? *Chem. Commun.* **2013**, *49*, 6256−6258.
(34) Li, S. S.; Northrop, B. H.; Yuan, Q. H.; Wan, L. J.; Stang, P. J. Surface confined metallosupramolecular architectures: Formation and scanning tunneling microscopy characterization. *Acc. Chem. Res.* **2009**, *42*, 249−259.
(35) Sakamoto, R.; Katagiri, S.; Maeda, H.; Nishihara, H. Bis(terpyridine) metal complex wires: Excellent long-range electron transfer ability and controllable intrawire redox conduction on silicon electrode. *Coord. Chem. Rev.* **2013**, *257*, 1493−1506.
(36) Nishimori, Y.; Kanaizuka, K.; Murata, M.; Nishihara, H. Synthesis of molecular wires of linear and branched bis(terpyridine)-complex oligomers and electrochemical observation of through-bond redox conduction. *Chem.—Asian J.* **2007**, *2*, 367−376.
(37) Tuccitto, N.; Ferri, V.; Cavazzini, M.; Quici, S.; Zhavnerko, G.; Licciardello, A.; Rampi, M. A. Highly conductive similar to ~ 40-nm-long molecular wires assembled by stepwise incorporation of metal centres. *Nat. Mater.* **2009**, *8*, 41−46.
(38) Gao, S.; Huang, Y.; Cao, M.; Liu, T.-f.; Cao, R. The fabrication of palladium-pyridyl complex multilayers and their application as a catalyst for the heck reaction. *J. Mater. Chem.* **2011**, *21*, 16467−16472.
(39) Liang, Y. W.; Schmehl, R. H. Coordination chemistry at a surface - polymetallic complexes prepared on quartz by alternate deposition of iron(II) and ruthenium(II) centers. *J. Chem. Soc., Chem. Commun.* **1995**, 1007−1008.
(40) Mondal, P. C.; Yekkoni Lakshmanan, J.; Hamoudi, H.; Zharnikov, M.; Gupta, T. Bottom-up assembly of multicomponent coordination-based oligomers. *J. Phys. Chem. C* **2011**, *115*, 16398−16404.
(41) Motiei, L.; Sassi, M.; Kaminker, R.; Evmenenko, G.; Dutta, P.; Iron, M. A.; van der Boom, M. E. Synergism in multicomponent self-propagating molecular assemblies. *Langmuir* **2011**, *27*, 1319−1325.
(42) Tsukruk, V. V.; Rinderspacher, F.; Bliznyuk, V. N. Self-assembled multilayer films from dendrimers. *Langmuir* **1997**, *13*, 2171−2176.
(43) Porcel, C.; Lavalle, P.; Ball, V.; Decher, G.; Senger, B.; Voegel, J.-C.; Schaaf, P. From exponential to linear growth in polyelectrolyte multilayers. *Langmuir* **2006**, *22*, 4376−4383.
(44) Denisevich, P.; Willman, K. W.; Murray, R. W. Unidirectional current flow and charge state trapping at redox polymer interfaces on bilayer electrodes - principles, experimental demonstration, and theory. *J. Am. Chem. Soc.* **1981**, *103*, 4727−4737.
(45) Hatzor, A.; Weiss, P. S. Molecular rulers for scaling down nanostructures. *Science* **2001**, *291*, 1019−1020.
(46) de Ruiter, G.; van der Boom, M. E. Sequential logic and random access memory (RAM): A molecular approach. *J. Mater. Chem.* **2011**, *21*, 17575−17581.

(47) de Ruiter, G.; van der Boom, M. E. Surface-confined assemblies and polymers for molecular logic. *Acc. Chem. Res.* **2011**, *44*, 563−573.
(48) Qian, D.-Y.; Nakamura, C.; Ishida, T.; Wenk, S.-O.; Wakayama, T.; Takeda, S.; Miyake, J. Palladium-mediated stepwise assembly of three-dimensional organized multiporphyrin arrays directly on solid substrates. *Langmuir* **2002**, 10237−10242.
(49) Ejima, H.; Richardson, J. J.; Liang, K.; Best, J. P.; van Koeverden, M. P.; Such, G. K.; Cui, J.; Caruso, F. One-step assembly of coordination complexes for versatile film and particle engineering. *Science* **2013**, *341*, 154−157.
(50) Kaminker, R.; de Hatten, X.; Lahav, M.; Lupo, F.; Gulino, A.; Evmenenko, G.; Dutta, P.; Browne, C.; Nitschke, J. R.; van der Boom, M. E. Assembly of surface-confined homochiral helicates: Chiral discrimination of dopa and unidirectional charge transfer. *J. Am. Chem. Soc.* **2013**, *135*, 17052−17059.